Astronomy & Astrophysics manuscript no. beir9101
(DOI: will be inserted by hand later)
February 3, 2008

Observations of $\mathrm{H}\alpha$, iron, and oxygen lines in B, Be, and shell stars

S. M. Saad[1,2], J. Kubát[1], D. Korčáková[1], P. Koubský[1], P. Škoda[1], M. Šlechta[1], A. Kawka[1], A. Budovičová[1], V. Votruba[3,1], L. Šarounová[1], M. I. Nouh[2]

[1] Astronomický ústav, Akademie věd České republiky, CZ-251 65 Ondřejov, Czech Republic
[2] National Research Institute of Astronomy and Geophysics, 11421 Helwan, Cairo, Egypt
[3] Ústav teoretické fyziky a astrofyziky PřF MU, Kotlářská 2, CZ-611 37 Brno, Czech Republic

Received 23 August 2004 / Accepted 21 December 2005

Abstract. We have carried out a spectroscopic survey of several B, Be, and shell stars in optical and near-infrared regions. Line profiles of the $\mathrm{H}\alpha$ line and of selected Fe II and O I lines are presented.

Key words. Stars: Be – line: profiles

1. Introduction

Observations of B, Be, and shell stars in different spectral regions are important for putting constraints on modeling these stars. Echelle spectrographs as well as the high sensitivity of modern detectors in the red part of the spectrum provide a wealth of the information contained in the whole visible and near infrared regions obtained simultaneously. The aim of this paper is a spectroscopic survey of line profiles of $\mathrm{H}\alpha$ and selected non-hydrogenic lines of iron and oxygen in the visual and near infrared region for selected bright B and Be stars. We mainly use the echelle observations secured using the *HEROS* (*H*eidelberg *E*xtended *R*ange *O*ptical *S*pectrograph) spectrograph attached to the Ondřejov 2m telescope supplemented by several CCD coudé spectra.

2. Observations and data reduction

The present data are based on new spectroscopic observations of 13 B stars, 28 Be stars, and 8 shell stars. Our sample of stars contains objects of spectral types B0 – B9.5 and luminosity classes III, IV and V. Table 1 summarises the basic information about the observed objects, their HD and HR no's, their name (if available), MK spectral type, luminosity class, and Julian dates of the observations. Some of these stars have never been observed before (to the best of our knowledge) in the near-infrared region. The spectra of these stars were obtained between January 2001 and November 2003 using the fiber-fed echelle spectrograph *HEROS* (for a brief description see Štefl & Rivinius 2000, Škoda & Šlechta 2002a) attached to the Cassegrain focus of the 2m telescope at Ondřejov Observatory.

Send offprint requests to: J. Kubát,
e-mail: `kubat@sunstel.asu.cas.cz`

All the basic data reduction processing, including bias subtraction, flat fielding, and wavelength calibration, have been done using the *HEROS* pipeline written by O. Stahl and A. Kaufer as an extension of basic MIDAS echelle context (see Stahl et al 1995, also Škoda & Šlechta 2002b). Additional observations of several stars were secured using a CCD detector of a coudé spectrograph of the same telescope (Šlechta & Škoda 2002) and the data were reduced by the IRAF package.

3. Observed lines

3.1. The hydrogen $\mathrm{H}\alpha$ line

The $\mathrm{H}\alpha$ line in the stars of our sample was found to be either in absorption or in emission, however, an intermediate case between emission and absorption was also found. Our set of stars exhibits basically five different shapes of $\mathrm{H}\alpha$ line. We introduce corresponding stellar subclasses for our sample, namely

i. Emission is present, but it is completely below the continuum level. We will denote this subclass as AbEm (absorption with emission).
ii. The absorption part is below the level of continuum while the emission peak is above the continuum. The ratio of these two parts often varies at different phases for the same star. We will denote this subclass as EmAb (emission with absorption).
iii. The whole emission feature is completely above the continuum level. They will be denoted by Em (pure emission).
iv. We may also define the shell stars characterised by extremely sharp $\mathrm{H}\alpha$ absorption cores as one of the Be star phases. Since there is no intrinsic difference between Be and shell stars, we denoted them by Sh. Besides the shape of the $\mathrm{H}\alpha$ emission line profile, the presence of other sharp

Table 1. List of the B and Be stars in our sample. References to the spectral type are denoted by superscript numbers in parentheses, and the values of $T_{\rm eff}$ are from Theodossiou & Danezis (1991).

HD	HR	Name	Sp. Type	$T_{\rm eff}$	JD–24 00 000	JD–24 00 000	Shape
22780	1113		B6V[(1)]	12915 ± 393	53217.5656	53217.5434	AbEm
23302	1142	17 Tau	B6III[(1)]	13810 ± 383	52619.9573		AbEm
36408B	1847B		B7IV[(4)]	12940 ± 1230	52721.8196		AbEm
217675	8762	o And	B6III[(1)]	13810 ± 383	51779.0595		AbEm
144	7	10 Cas	B9III[(1)]	10700 ± 385	52931.3284	53204.5171	EmAb
6811	335	ϕ And	B7III[(1)]	12940 ± 1230	52566.8285		EmAb
58050	2817	OT Gem	B2V[(1)]	22400 ± 1393	52697.9049		EmAb
58715	2845	β CMi	B8Vn[(1)]	12120 ± 623	52620.0981		EmAb
164447	6720	V974 Her	B8Vn[(1)]	12120 ± 623	53215.4018	53215.4485	EmAb
171780	6984		B6V[(1)]	15310 ± 750	53070.6629	53182.4968	EmAb
200310	8053	60 Cyg	B1V[(1)]	25570 ± 3652	52567.9192		EmAb
205021	8238	β Cep	B2III[(5)]	22160 ± 1145	52113.0762		EmAb
216200	8690	V360 Lac	B3III[(2)]	18445 ± 1426	52527.0736		EmAb
4180	193	o Cas	B5III[(1)]	15310 ± 750	52694.8389		Em
5394	264	γ Cas	B0.5IV[(1)]	30025 ± 2160	52682.7532		Em
10516	496	ϕ Per	B1.5(V:)e-sh[(2)]	25570 ± 3652	52465.0435		Em
18552	894		B7IVe[(2)]	12120 ± 623	51954.7961		Em
22192	1087	ψ Per	B3IIIe-sh[(2)]	15310 ± 750	53216.5315	53216.4905	Em
23630	1165	η Tau	B7IIIe[(2)]	12940 ± 1230	52648.8068		Em
29866	1500		B7IV[(1)]	12120 ± 623	52526.1050		Em
109387	4787	κ Dra	B5IIIe[(2)]	15310 ± 750	52720.9752		Em
175863		BD+59 1929	B4Ve [(3)]	17100 ± 386	53182.4428	53182.4642	Em
193911	7789	25 Vul	B6IVe[(2)]	14340 ± 570	52525.9284		Em
200120	8047	59 Cyg	B1Ve[(2)]	25340 ± 2164	51795.9049		Em
203467	8171	6 Cep	B2.5Ve[(2)]	18445 ± 1426	52721.0674		Em
206773		BD+57°2374	B0V:pe[(5)]	29230 ± 208	52484.0447		Em
217891	8773	β Psc	B5Ve[(2)]	15310 ± 750	53216.5717	53216.5525	Em
		EE Cep	B5:neβ[(13)]		53217.5020	53217.4567	Em
23862	1180	28 Tau	B8(V:)e-sh[(2)]	12120 ± 623	51797.0884		Sh
37202	1910	ζ Tau	B1IVe-sh[(2)]	25570 ± 3652	51897.9234		Sh
50658	2568	ψ^9 Aur	B6IV[(2)]	12300 ± 945	52721.9337		Sh
142926	5938	4 Her	B7IVe-sh[(2)]	12300 ± 945	52488.8992		Sh
162732	6664	88 Her	B7Vn[(1)]	12915 ± 393	53217.4040	53217.4229	Sh
171406	6971	V532 Lyr	B5V[(1)]	17100 ± 386	53182.3954	53182.4168	Sh
179343		BD+02°3815	B9V[(1)]	10580 ± 373	53216.4505	53216.4034	Sh
217050	8731	EW Lac	B3IVe-sh[(2)]	18445 ± 1426	53217.3848	53217.3731	Sh
358	15	α And	B9p[(11)]	10700 ± 385	51779.1187		Ab
886	39	γ Peg	B2IV[(3)]	22400 ± 1393	51771.0511		Ab
23873		BD+23°561	B9.5V[(12)]	10340 ± 465	52651.0012		Ab
24760	1220	ϵ Per	B0.5V[(5)]	30000	52648.7495		Ab
34759	1749	ρ Aur	B3V[(7)]	15310 ± 750	52351.9306		Ab
36408	1847A		B7III[(4)]	12940 ± 1230	52720.8740		Ab
44743	2294	β CMa	B1II/III[(5)]	26105 ± 1779	52720.7954		Ab
87901	3982	α Leo	B7Vn[(6)]	12120 ± 623	51925.0219		Ab
120315	5191	η UMa	B3V[(7)]	18445 ± 1426	52618.2262		Ab
138749	5778	θ CrB	B6Vn[(1)]	14340 ± 570	52693.1422		Ab
155763	6396	ζ Dra	B7III[(8)]	13810 ± 383	52002.1433		Ab
160762	6588	ι Her	B3V SB[(9)]	18445 ± 1426	51787.9064		Ab
164852	6738	96 Her	B3IV[(10)]	18445 ± 1426	52722.1490		Ab

References: (1) – Jaschek et al. (1980); (2) – Slettebak (1982); (3) – SIMBAD; (4) – Levato (1975); (5) – Morgan et al. (1955); (6) – Murphy

photospheric absorption lines which will be referred to as "shell lines" were also used for defining this subgroup.

v. The last subclass consists of normal B stars with Hα absorption lines. They are included in our analysis as a kind of standard star. We denote them by Ab.

Our five subclasses represent a qualitative estimate of the Hα line profile in our *present* observations. Table 1 lists the stars according to these subclasses.

3.2. Non-hydrogen emission lines

There is a number of non-hydrogen emission lines in the spectra of Be stars. The most striking emission features are produced by iron, helium, and oxygen. In addition to the hydrogen lines, these non-hydrogenic lines carry supplementary information coming from different regions of the stellar envelope depending on their depth of formation.

3.2.1. Iron lines

Iron lines bring a lot of information from the circumstellar envelope depending on their depth of formation. They are often present in the spectra of Be stars. An interesting fact about Fe II lines is that they appear in the emission spectrum, however, in the approximate theoretical spectrum, which was calculated under the simplified assumption of a LTE static plane-parallel atmosphere, they are completely missing. This indicates that the excitation mechanism is connected more probably with the atomic structure of Fe II and the corresponding NLTE pumping than with some global density changes or even iron overabundance. However, such a conclusion is to be verified by detailed NLTE calculations. We selected several strong lines mostly from the quartet system for our measurements.

Although the list of available Fe II lines is quite long, only several of them are useful for further analysis, in particular the 4233 Å line from the multiplet (27), the 4584 Å line from the multiplet (38), 6148 and 6456 Å lines from the multiplet (74), and 7516 and 7712 Å lines from the multiplet (73). Note that the 6148 Å line itself is a blend of two neighbouring Fe II lines. Due to its vicinity to the Hα line the Fe II 6456 Å line was present in the Hα spectrograms that were obtained with the CCD coudé camera.

The near-infrared line Fe II 7712 Å was severely contaminated by telluric lines in the band 7600 – 7700 Å. However, this line was sometimes strong enough to be measurable in 13 stars of our sample. In ten of them the line was in emission. Other Fe II lines, namely the 7516, 6456, and 6148 Å lines are also in emission. However, another Fe II line, which is not listed in the multiplet tables of Moore (1972), appeared to be quite strong in the synthetic spectra and may be possibly misidentified with the Fe II 7516 Å line. This line has a wavelength of 7513.162 Å and arises from the transition $5s\ e\,^6\mathrm{D}^{\mathrm{e}}_{9/2} \rightarrow 5p\ w\,^6\mathrm{P}^{\mathrm{o}}_{7/2}$. For simplicity we will identify this feature with the wavelength 7516 Å in the figures. In most cases the iron line Fe II 6516 Å was not detectable due to the huge number of telluric lines.

Table 2. List presented Fe II line profiles. For all stars the Hα and O I 7772–5 Å lines are presented as well.

Star	4233	4584	5169	5235	5317	5363	6432	6456	7462	7516	7712
HR 1847B			+	+	+						
o And			+	+	+						
10 Cas								+			
ϕ And	+	+									
β CMi			+	+	+			+			+
V974 Her											+
o Cas	+	+	+	+	+					+	+
γ Cas	+	+	+	+	+					+	+
ϕ Per	+	+	+	+	+					+	+
HR 894			+	+	+						
ψ Per							+	+			+
HR 1500			+	+	+						
κ Dra	+	+	+	+	+	+		+		+	+
HD 175863								+			+
25 Vul			+	+	+						
59 Cyg										+	+
6 Cep	+	+	+	+	+			+		+	+
HD 206773										+	+
β Psc										+	+
EE Cep										+	+
28 Tau	+	+	+	+	+					+	+
ζ Tau	+	+	+	+	+					+	+
4 Her	+	+	+	+	+						+
88 Her								+			+
HD 179343											+
EW Lac								+		+	+
HD 23873											+
ρ Aur			+					+		+	
β CMa									+		
α Leo			+								
η UMa			+								
θ CrB			+								
ζ Dra	+	+	+	+	+			+			
ι Her			+	+	+						

3.2.2. The oxygen infrared triplet O I 7772–5 Å

The most dominant oxygen line in the visible and near infrared spectra of Be stars is the near IR triplet line at 7772, 7774, 7775 Å emerging from the transition $3s\ ^5\mathrm{S}^{\mathrm{o}} \rightarrow 3p\ ^5\mathrm{P}$. Other transitions between quintet levels which fall into the visual region are missing in the spectra.

4. Description of the online material

Results of our observations are plotted in the online Appendix. It contains an atlas of the individual line profiles sorted and ordered according to the Table 1. For each star, the Hα and O I 7772–5 Å lines are plotted. Iron lines are plotted for each observation where they were available. The list of Fe II lines presented is listed in the Table 2.

Acknowledgements. This research has made use of the NASA's Astrophysics Data System Abstract Service (Kurtz et al. 2000, Eichhorn et al. 2000, Accomazzi et al. 2000, Grant et al. 2000). Our work was supported by grants of the Grant Agency of the

Czech Republic 205/02/0445 and 102/02/1000. Astronomical Institute Ondřejov is supported by a project Z10030501.

References

Accomazzi, A., Eichhorn, G., Kurtz, M. J., Grant, C. S., & Murray, S. S. 2000, A&AS 143, 85
Cowley, A. Cowley, C., Jaschek, M., & Jaschek, C. 1969, AJ, 74, 375.
Eichhorn, G., Kurtz, M. J., Accomazzi, A., Grant, C. S., & Murray, S. S. 2000, A&AS, 143, 61
Grant, C. S., Accomazzi, A., Eichhorn, G., Kurtz, M. J., & Murray, S. S. 2000, A&AS 143, 111
Herbig, G. H. 1960, ApJ 131, 632
Jaschek, M., Hubert-Delplace, A. M., Hubert, H. & Jaschek, C. 1980, A&AS, 42, 103
Johnson, H. L., & Morgan, W. W. 1953, ApJ, 117, 313
Kurtz, M. J., Eichhorn, G., Accomazzi, A. et al. 2000, A&AS, 143, 41
Lesh, J. R. 1968, ApJS, 17, 371
Levato, H. 1975, A&AS, 19, 91
Mendoza, V. E. E. 1956, ApJ, 123, 54
Molnar, M. R. 1972, ApJ, 175, 453
Morgan, W. W., Code, A. C., & Whitford, A. E. 1955, ApJS, 2, 41.
Morgan, W. W. & Keenan, P. C. 1973, ARA&A, 11, 29
Moore, C. E., 1972, A Multiplet Table of Astrophysical Interest, NSRDS-NBS 40
Murphy, R. E. 1969, AJ, 74, 1082
Škoda, P., & Šlechta, M. 2002a, Publ. Astron. Inst. Czech 90, 1
Škoda, P., & Šlechta, M. 2002b, Publ. Astron. Inst. Czech 90, 40
Šlechta, M., & Škoda, P. 2002, Publ. Astron. Inst. Czech 90, 9
Slettebak, A. 1982, ApJS 50, 55
Stahl, O., Kaufer, A., Wolf, B. et al. 1995, J. Astron. Data 1, 3
Štefl, S., & Rivinius, T. 2000, in The Be Phenomenon in Early Type Stars, IAU Coll. 175, M. A. Smith, H. F. Henrichs, & J. Fabregat eds., ASP Conf. Ser. Vol. 214, p. 356
Theodossiou, E. & Danezis, E. 1991, Ap&SS, 183, 91

Online Material

Appendix A: Atlas of individual line profiles

Note that the panels which contain more than one profile the spectra are arbitrarly shifted by 0.2, 0.4 and 0.6 below or above the continuum level.

A.1. AbEm *subclass*

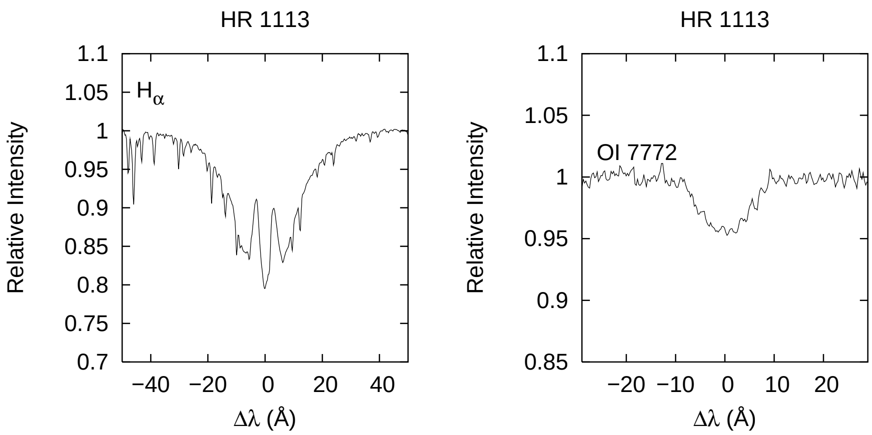

Fig. A.1. Profiles of Hα and O I 7772−5 Å lines of HR 1113.

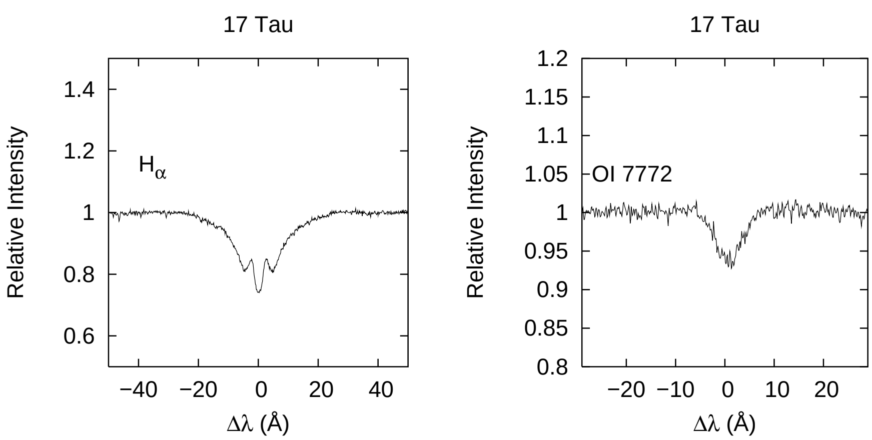

Fig. A.2. Profiles of Hα and O I 7772−5 Å lines of 17 Tau.

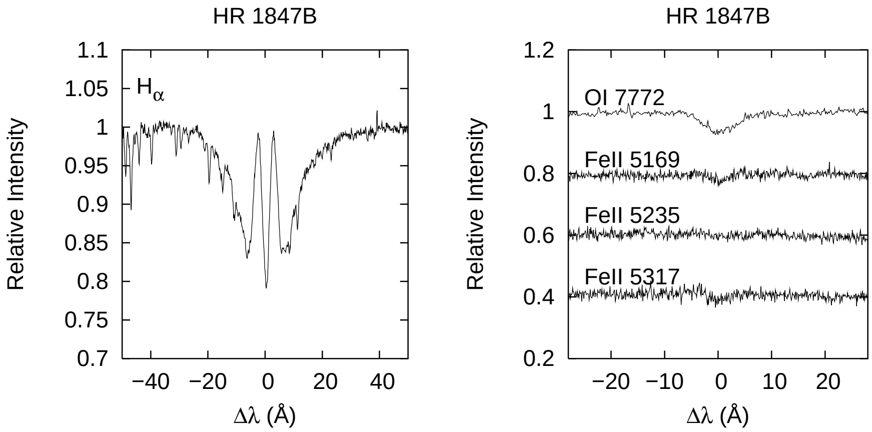

Fig. A.3. Profiles of Hα, Fe II 5169, 5235, 5317 Å, and O I 7772−5 Å lines of HR 1847B.

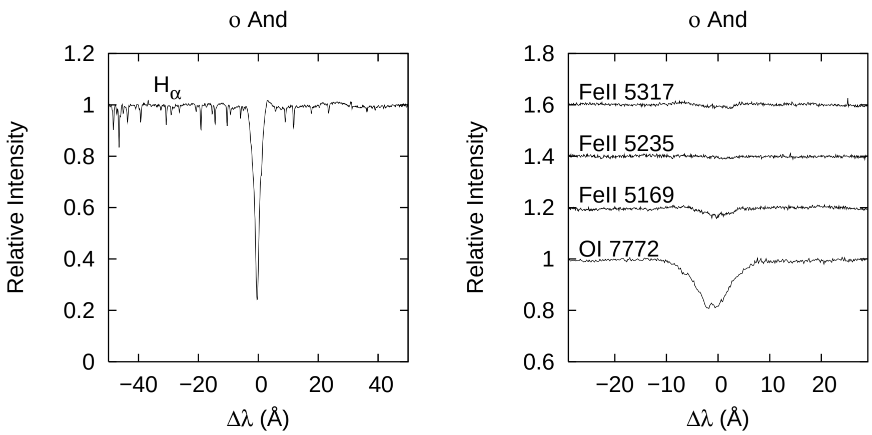

Fig. A.4. Profiles of Hα, Fe II 5169, 5235, 5317 Å, and O I 7772−5 Å lines of *o* And.

A.2. EmAb *subclass*

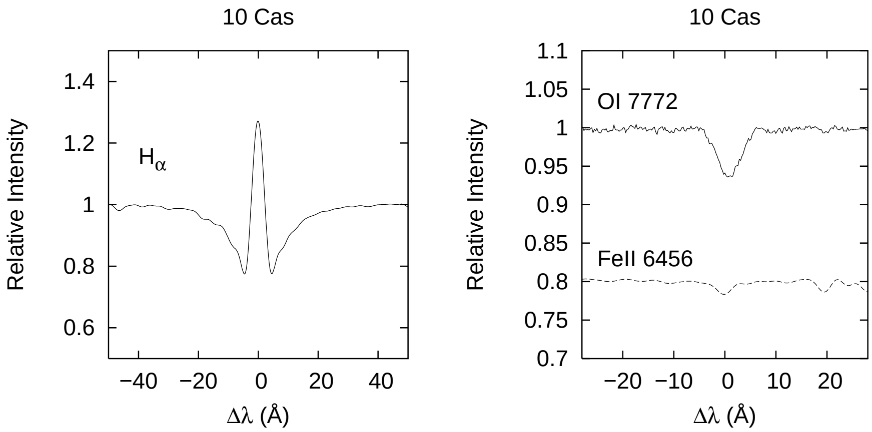

Fig. A.5. Profiles of Hα, Fe II 6456 Å, and O I 7772−5 Å lines of 10 Cas.

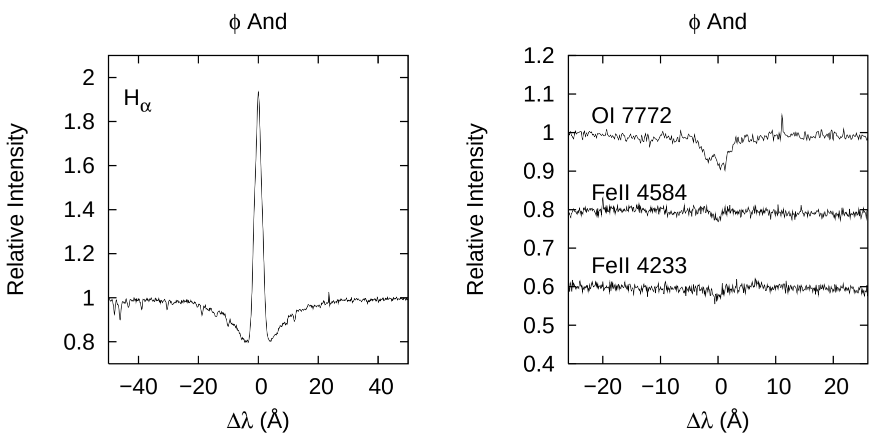

Fig. A.6. Profiles of Hα, Fe II 4233, 4584 Å, and O I 7772−5 Å lines of ϕ And.

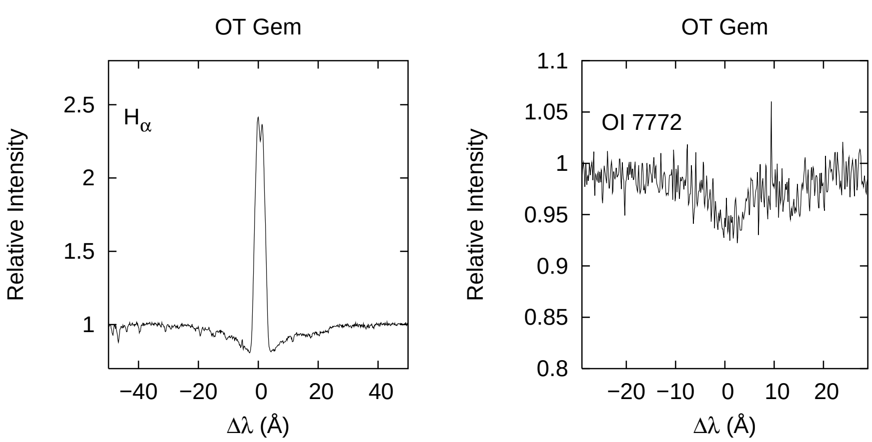

Fig. A.7. Profiles of Hα and O I 7772−5 Å lines of OT Gem.

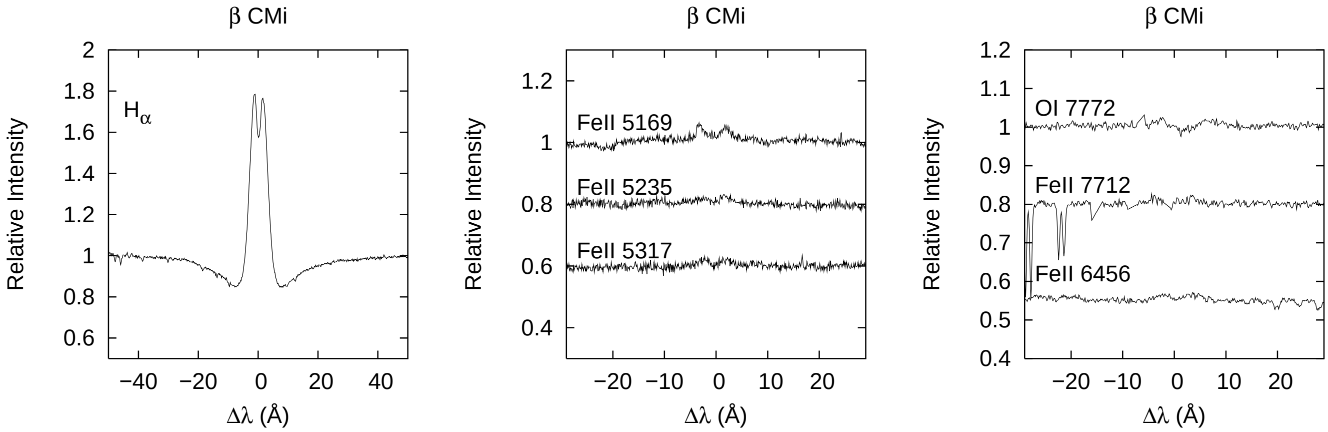

Fig. A.8. Profiles of Hα, Fe II 5169, 5235, 5317, 6456, 7712, and O I 7772−5 Å lines of β CMi.

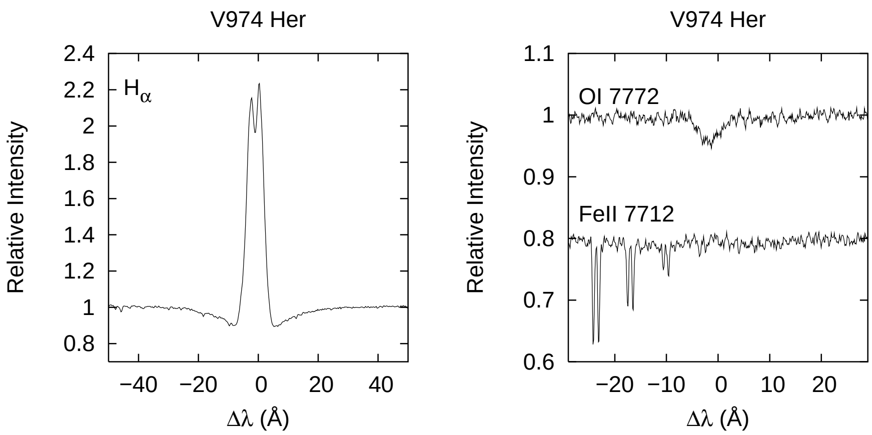

Fig. A.9. Profiles of Hα, Fe II 77712 Å, and O I 7772−5 Å lines of V974 Her (HD 164447).

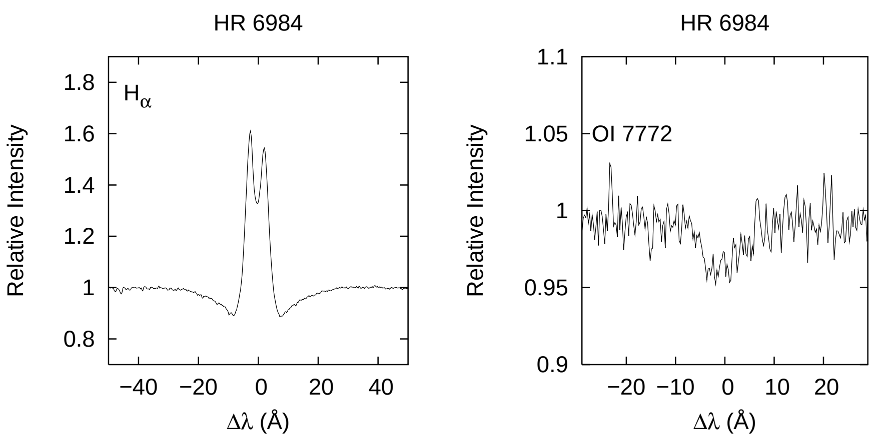

Fig. A.10. Profiles of Hα and O I 7772−5 Å lines of HR 6984 (HD 171780).

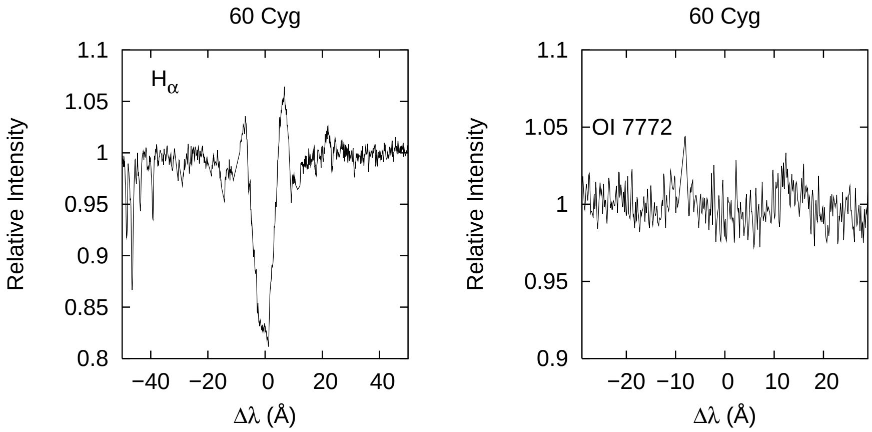

Fig. A.11. Profiles of Hα and O I 7772−5 Å lines of 60 Cyg.

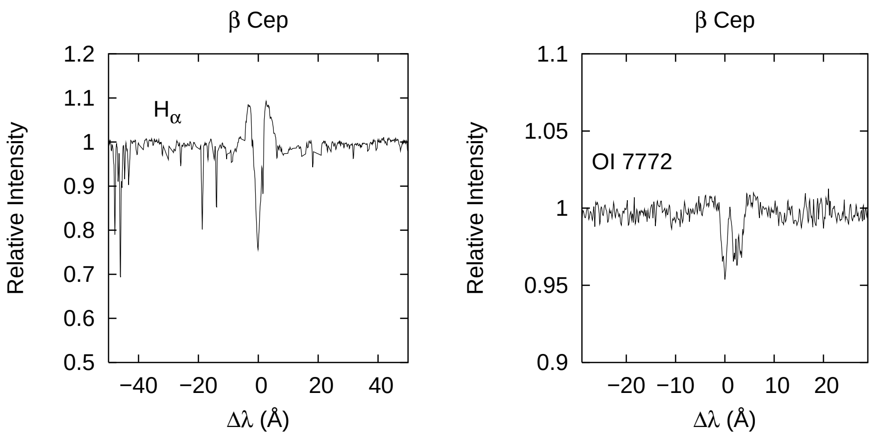

Fig. A.12. Profiles of Hα and O I 7772−5 Å lines of β Cep.

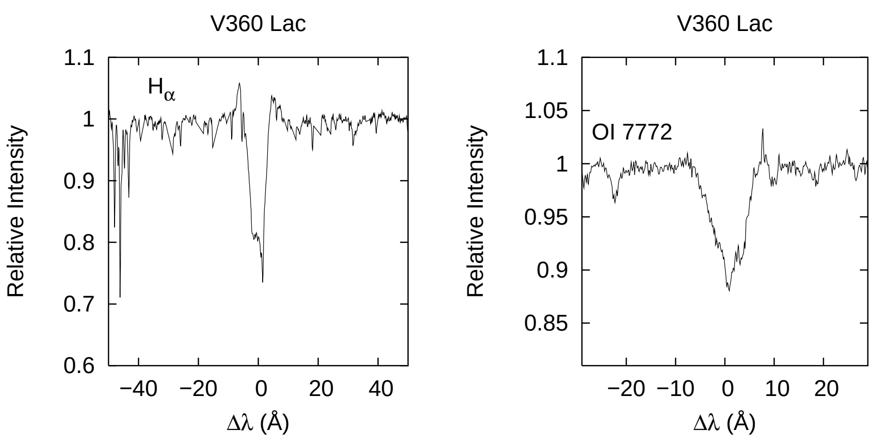

Fig. A.13. Profiles of Hα and O I 7772−5 Å lines of V 360 Lac.

A.3. Em *subclass*

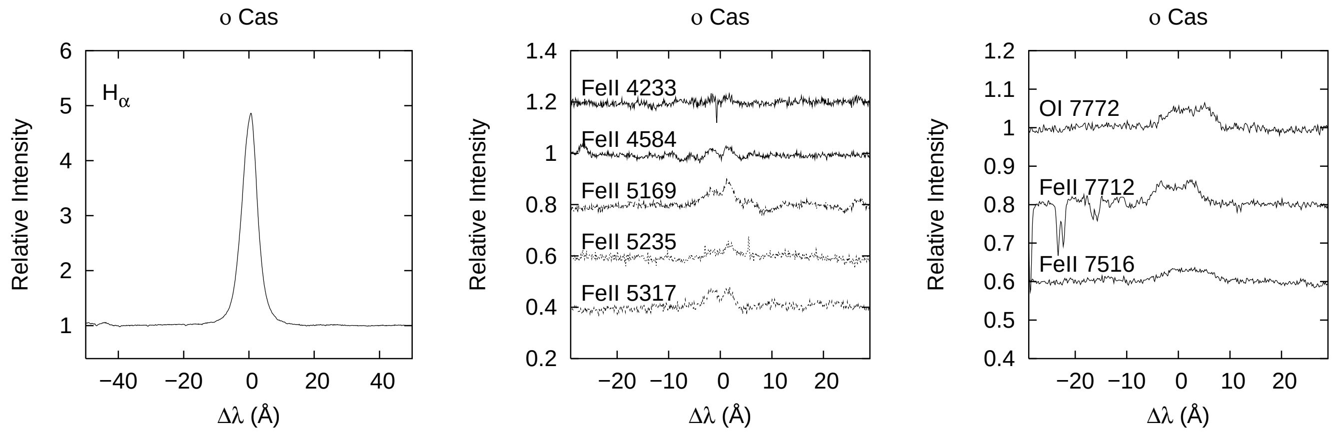

Fig. A.14. Profiles of Hα, Fe II 4233, 4584, 5169, 5235, 5317, 7516, 7712 Å, and O I 7772−5 Å lines of *o* Cas.

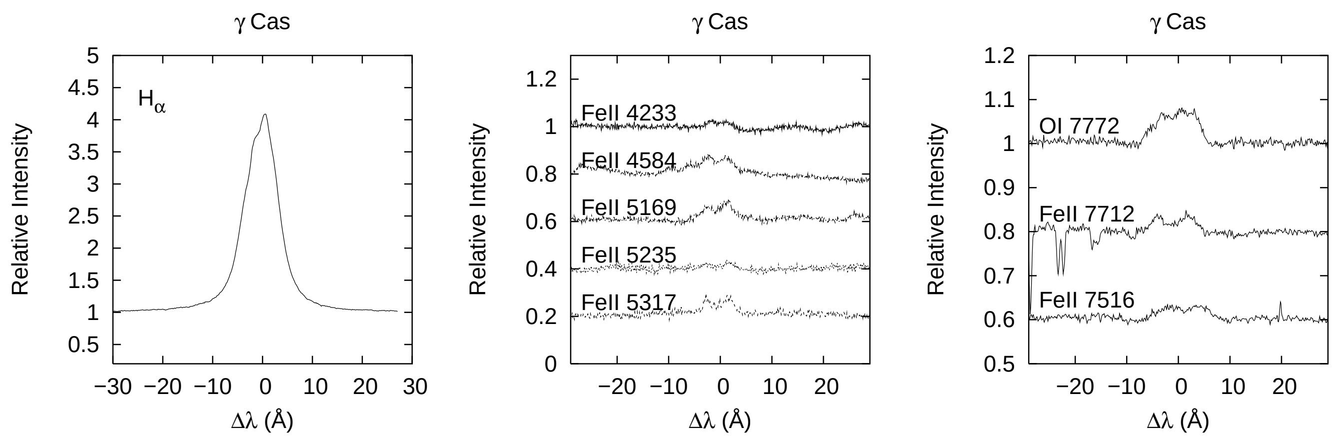

Fig. A.15. Profiles of Hα, Fe II 4233, 4584, 5169, 5235, 5317, 7516, 7712 Å, and O I 7772−5 Å lines of γ Cas.

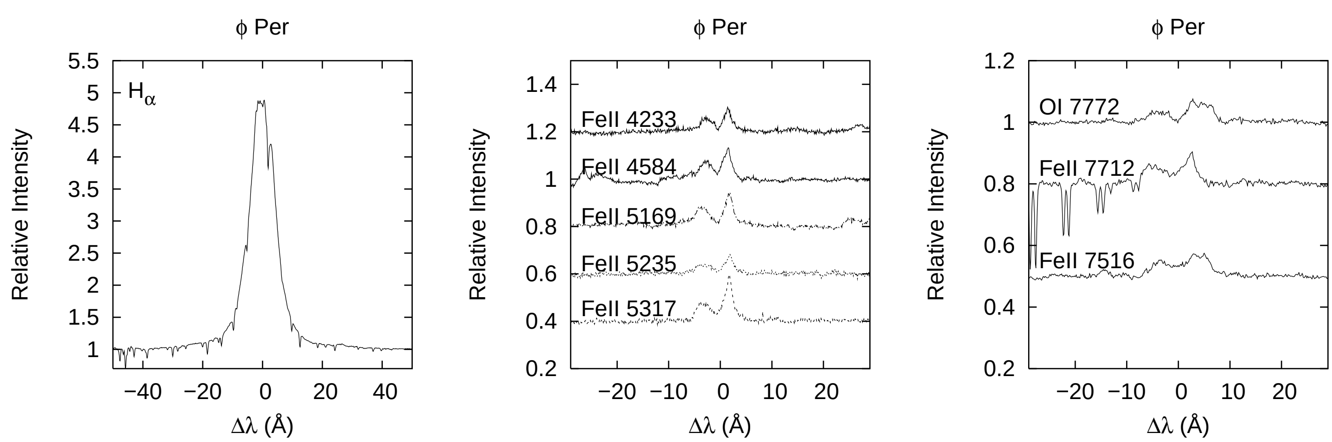

Fig. A.16. Profiles of Hα, Fe II 4233, 4584, 5169, 5235, 5317, 7516, 7712 Å, and O I 7772−5 Å lines of ϕ Per.

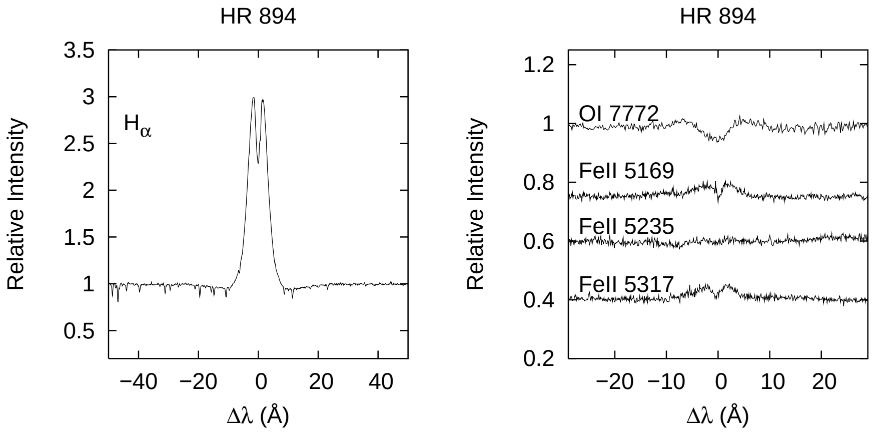

Fig. A.17. Profiles of Hα, Fe II 5169, 5235, 5317 Å, and O I 7772−5 Å lines of HR 894.

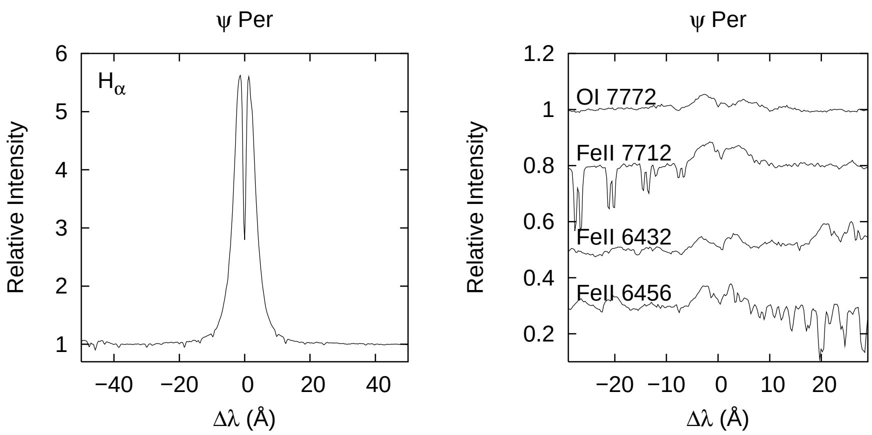

Fig. A.18. Profiles of Hα and Fe II 6432, 6456, 7712 Å lines of ψ Per.

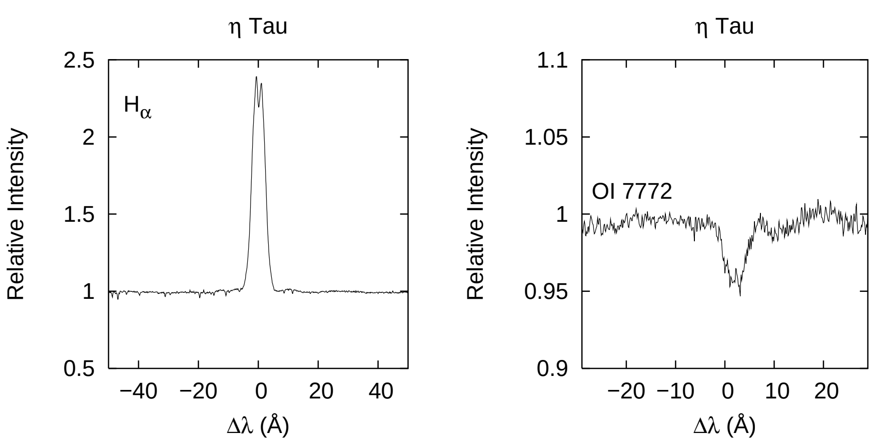

Fig. A.19. Profiles of Hα and O I 7772−5 Å lines of η Tau.

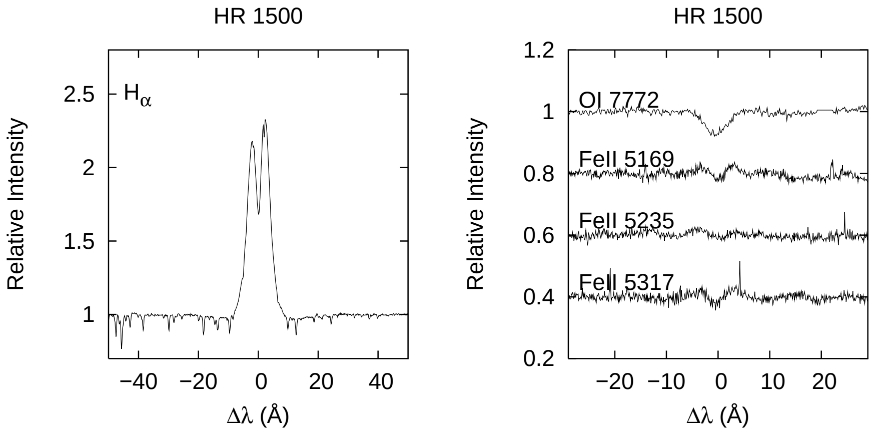

Fig. A.20. Profiles of Hα, Fe II 5169, 5235, 5317 Å, and O I 7772−5 Å lines of HR 1500.

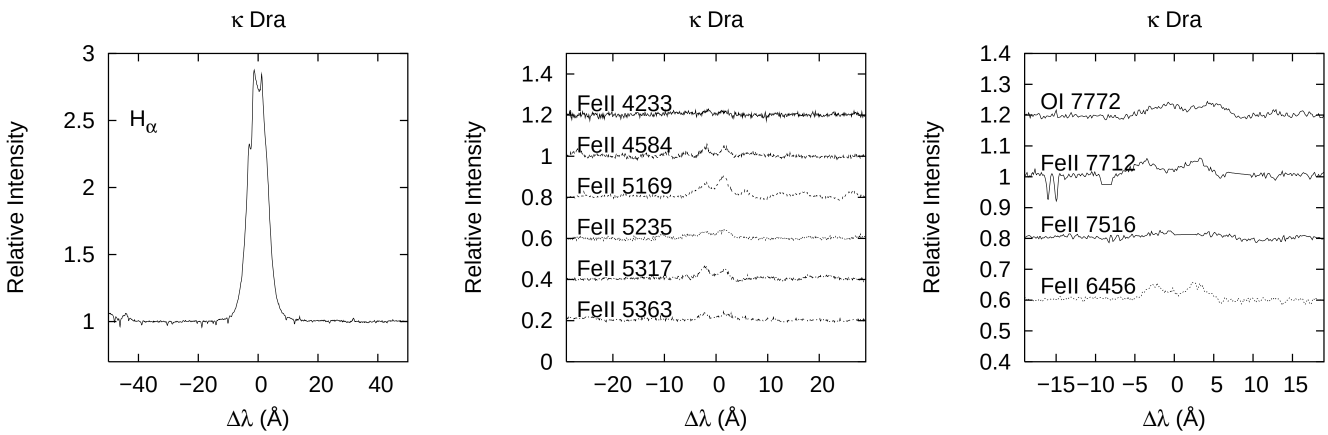

Fig. A.21. Profiles of Hα, Fe II 4233, 4584, 5169, 5235, 5317, 5363, 6456, 7516, 7712 Å, and O I 7772−5 Å lines of κ Dra.

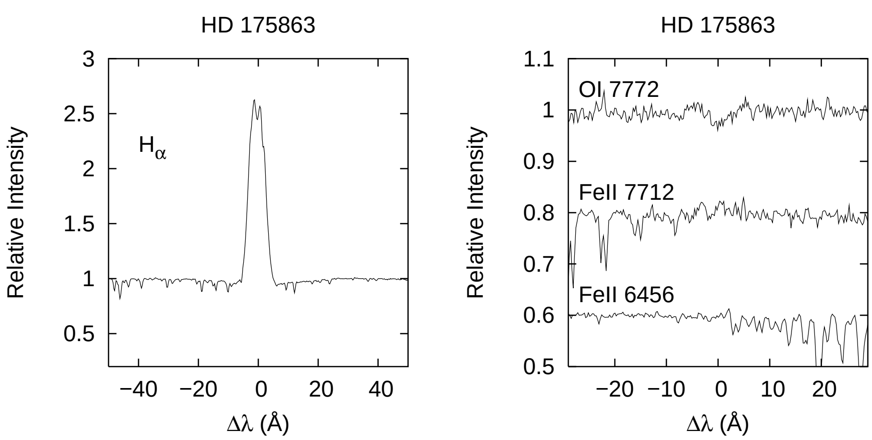

Fig. A.22. Profiles of Hα, Fe II 6456, 7712 Å, and O I 7772−5 Å lines of HD 175863.

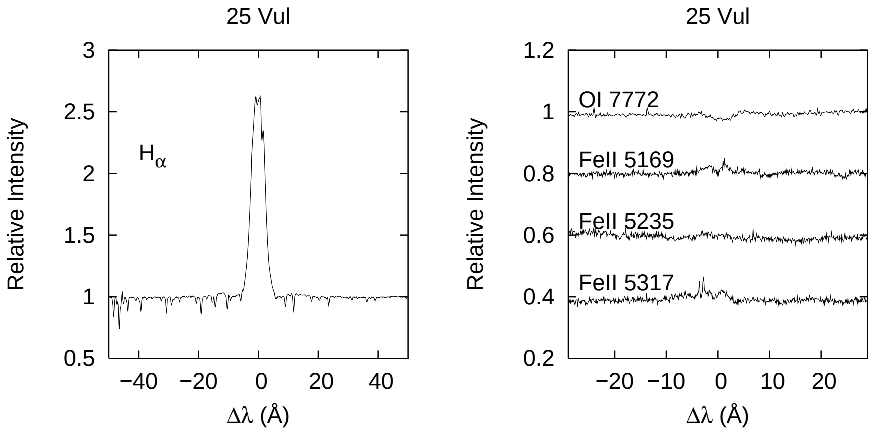

Fig. A.23. Profiles of Hα, Fe II 5169, 5235, 5317 Å, and O I 7772−5 Å lines of 25 Vul.

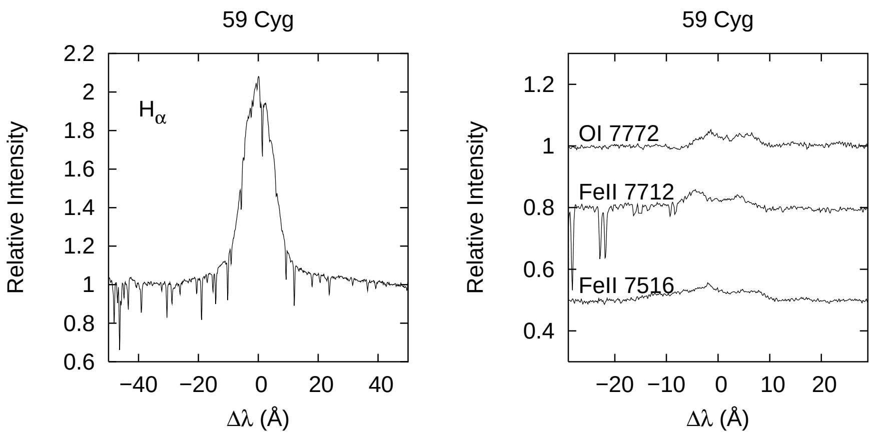

Fig. A.24. Profiles of Hα, Fe II 7516, 7712 Å, and O I 7772−5 Å lines of 59 Cyg.

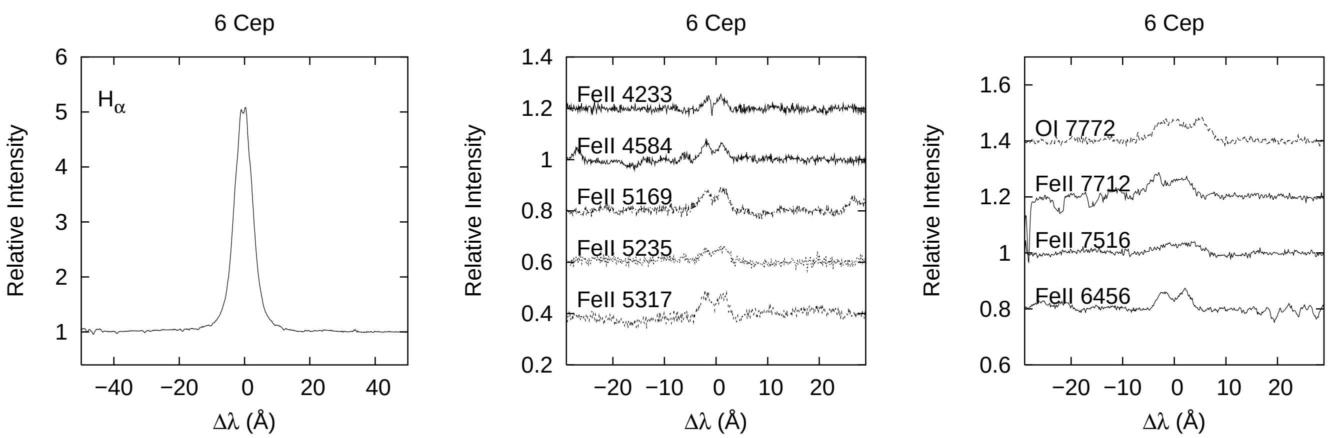

Fig. A.25. Profiles of Hα, Fe II 4233, 4584, 5169, 5235, 5317, 6456, 7516, 7712 Å, and O I 7772−5 Å lines of 6 Cep.

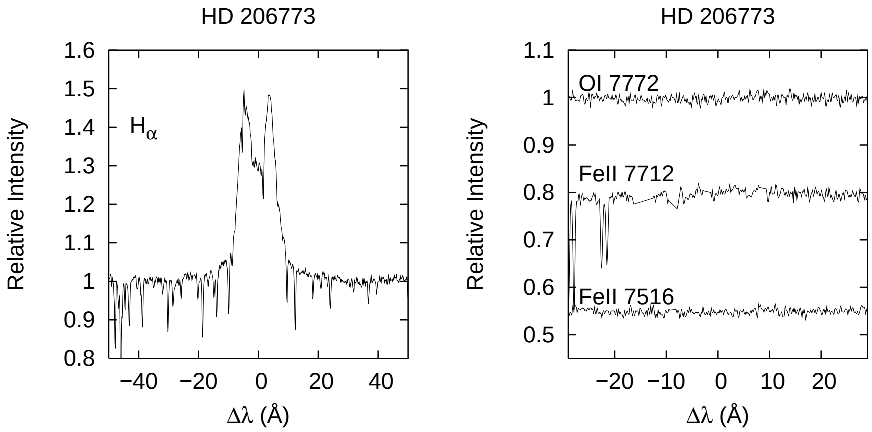

Fig. A.26. Profiles of Hα, Fe II 7516, 7712 Å, and O I 7772−5 Å lines of HD 206773.

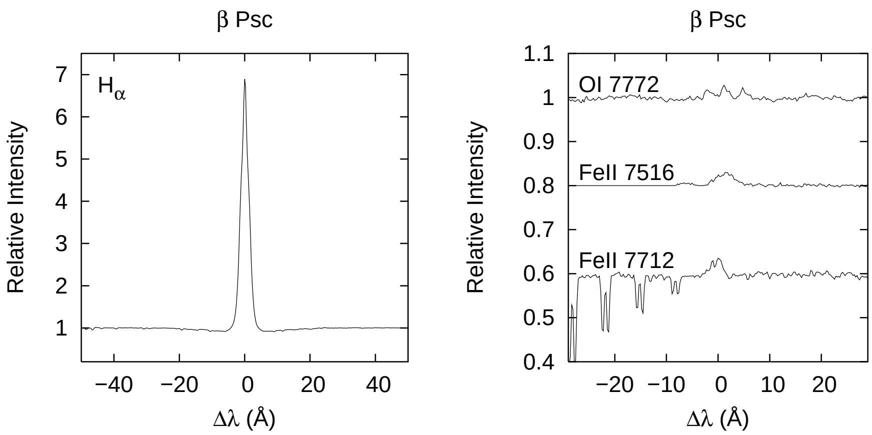

Fig. A.27. Profiles of Hα, Fe II 7516, 7712 Å, and O I 7772−5 Å lines of β Psc.

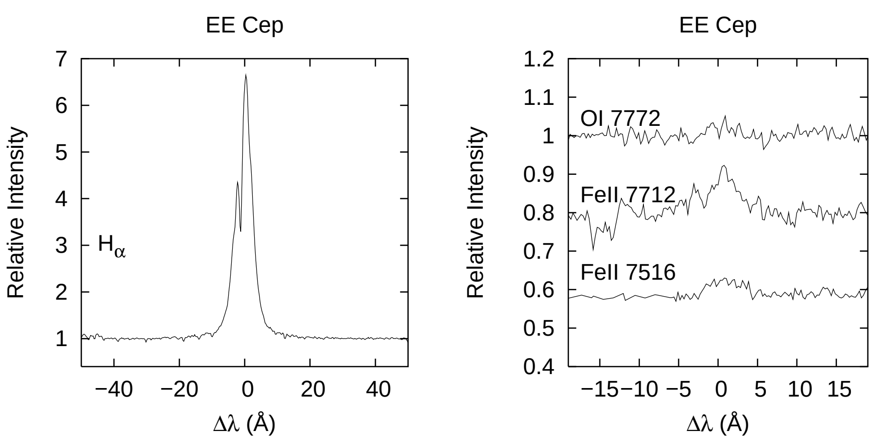

Fig. A.28. Profiles of Hα, Fe II 7516, 7712 Å, and O I 7772−5 Å lines of EE Cep.

A.4. Sh *subclass*

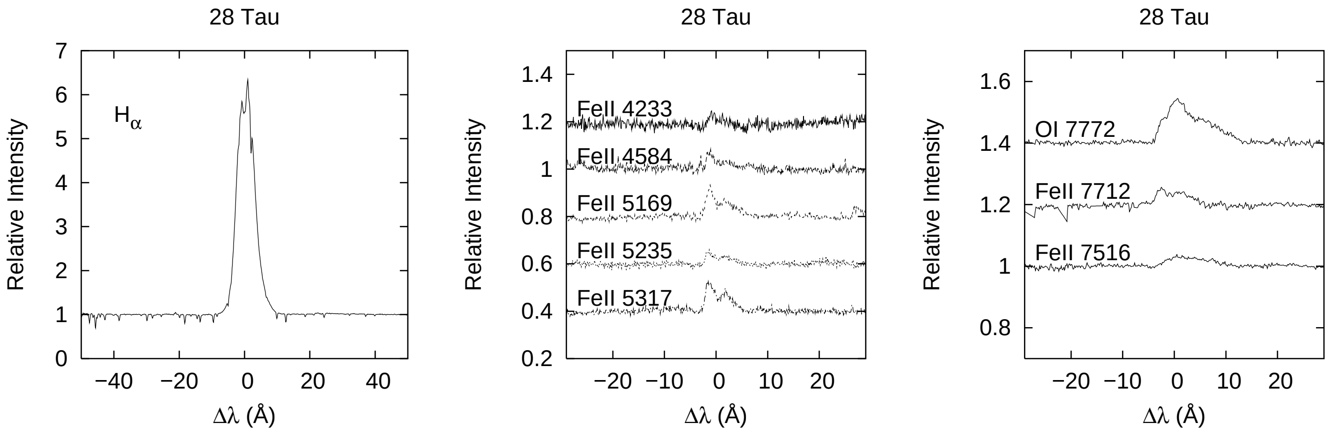

Fig. A.29. Profiles of Hα, Fe II 4233, 4584, 5169, 5235, 5317, 7516, 7712 Å, and O I 7772−5 Å lines of 28 Tau.

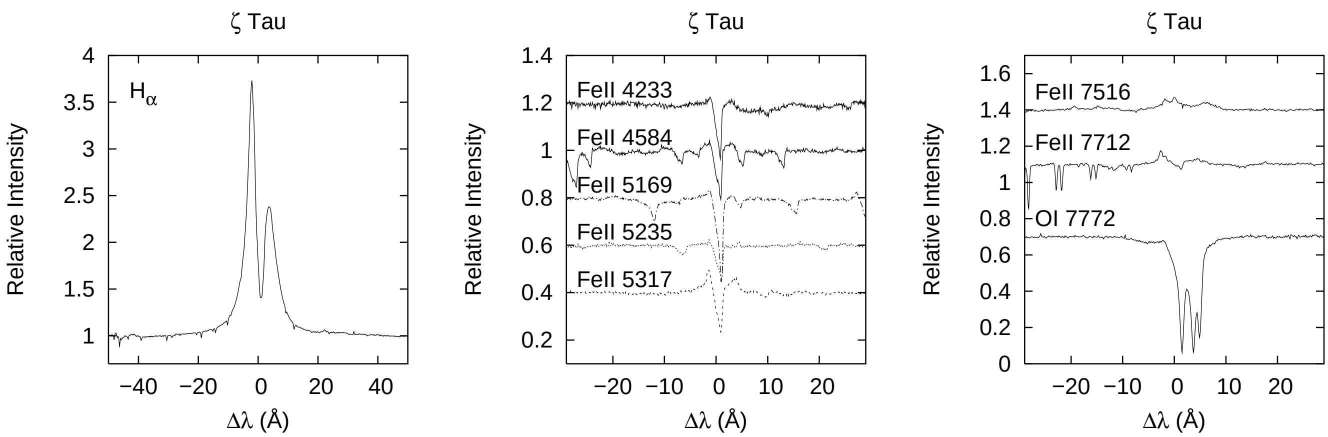

Fig. A.30. Profiles of Hα, Fe II 4233, 4584, 5169, 5235, 5317, 7516, 7712 Å, and O I 7772−5 Å lines of ζ Tau.

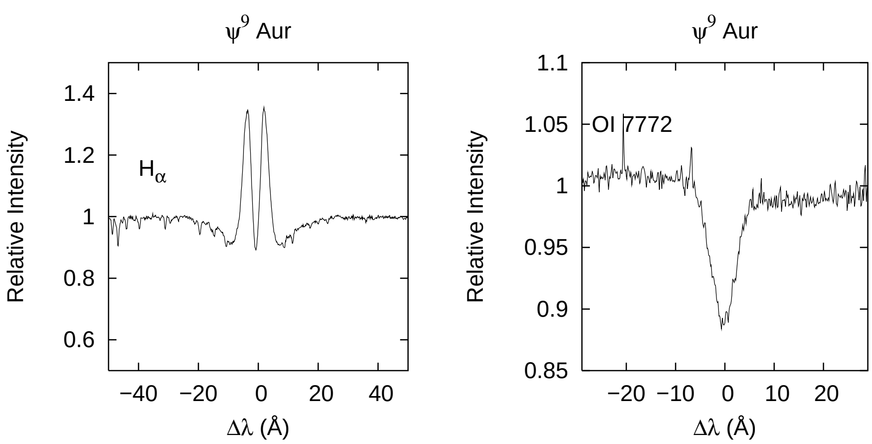

Fig. A.31. Profiles of Hα and O I 7772−5 Å lines of ψ^9 Aur.

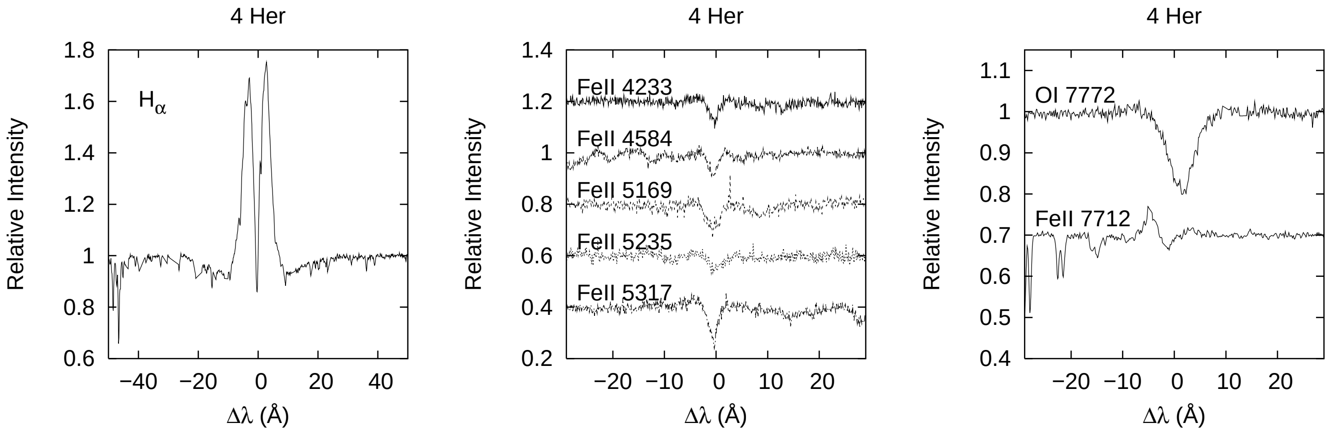

Fig. A.32. Profiles of Hα, Fe II 4233, 4584, 5169, 5235, 5317, 7712 Å, and O I 7772−5 Å lines of 4 Her.

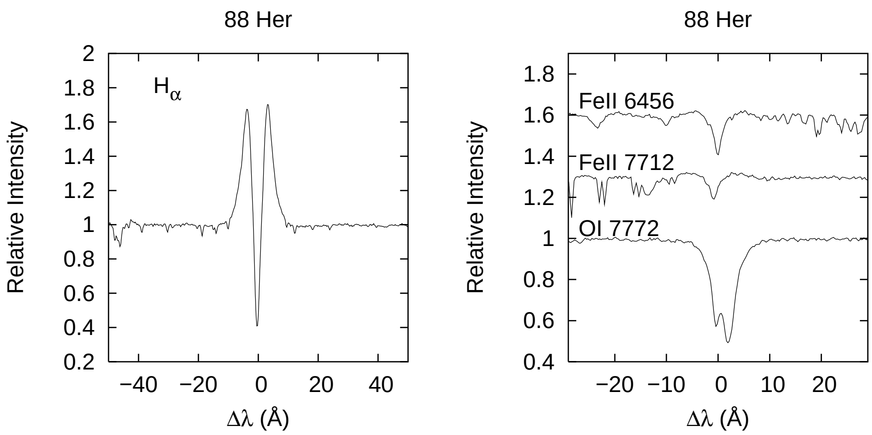

Fig. A.33. Profiles of Hα, Fe II 6456, 7712 Å, and O I 7772−5 Å lines of 88 Her.

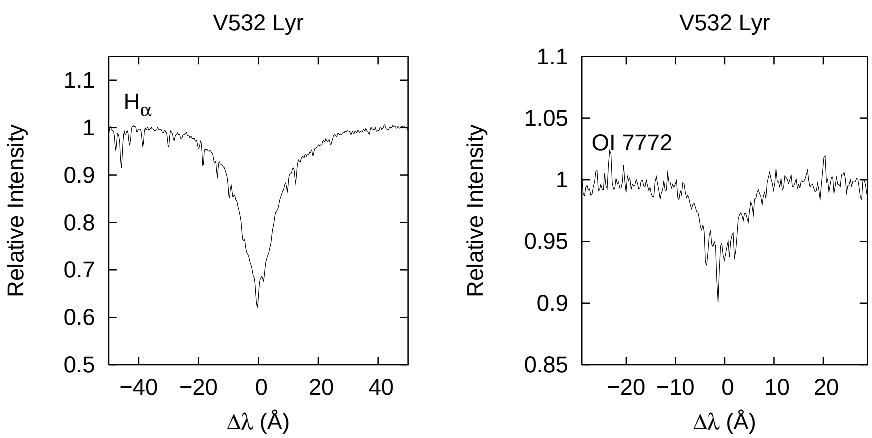

Fig. A.34. Profiles of Hα, Fe II 6516 Å, and O I 7772−5 Å lines of HR 6971 (HD 171406, V 532 Lyr).

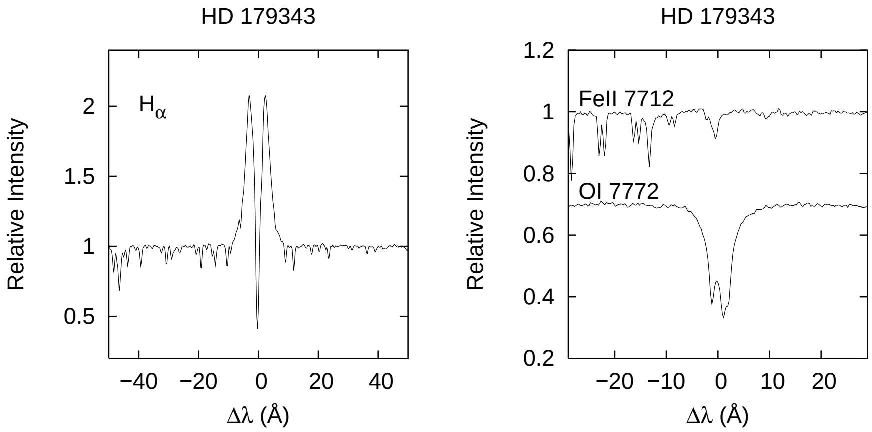

Fig. A.35. Profiles of Hα, Fe II 7712 Å, and O I 7772−5 Å lines of HD 179343.

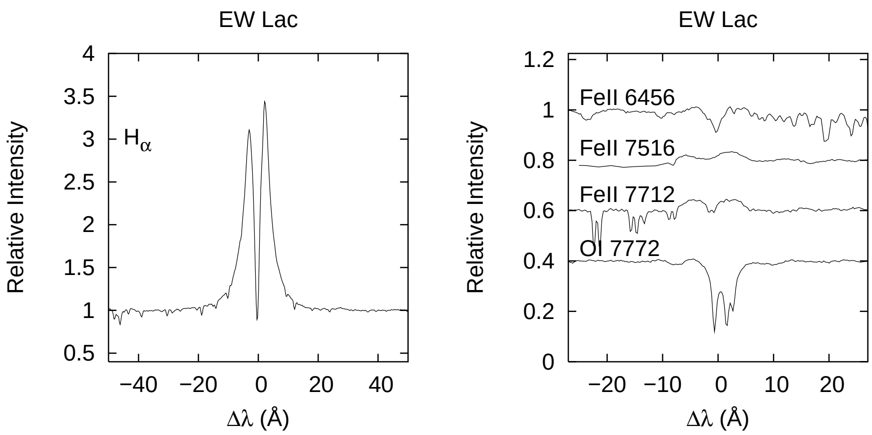

Fig. A.36. Profiles of Hα, Fe II 6456, 7516, 7712 Å, and O I 7772−5 Å lines of EW Lac.

A.5. Ab *subclass*

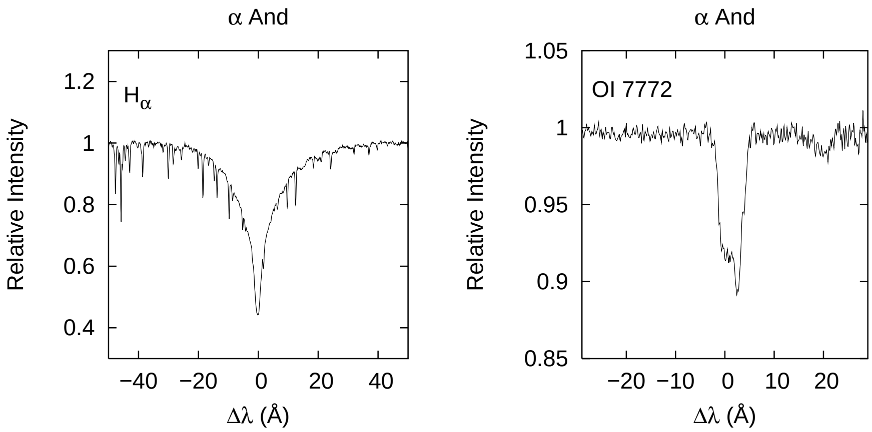

Fig. A.37. Profiles of Hα and O I 7772−5 Å lines of α And.

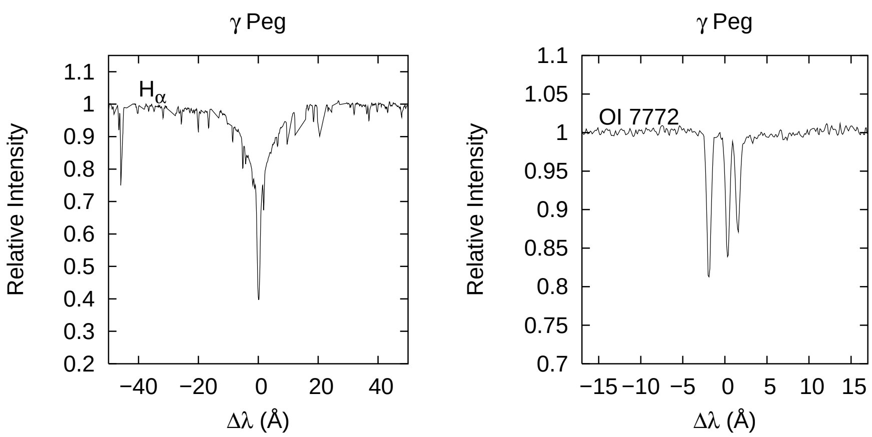

Fig. A.38. Profiles of Hα and O I 7772−5 Å lines of γ Peg.

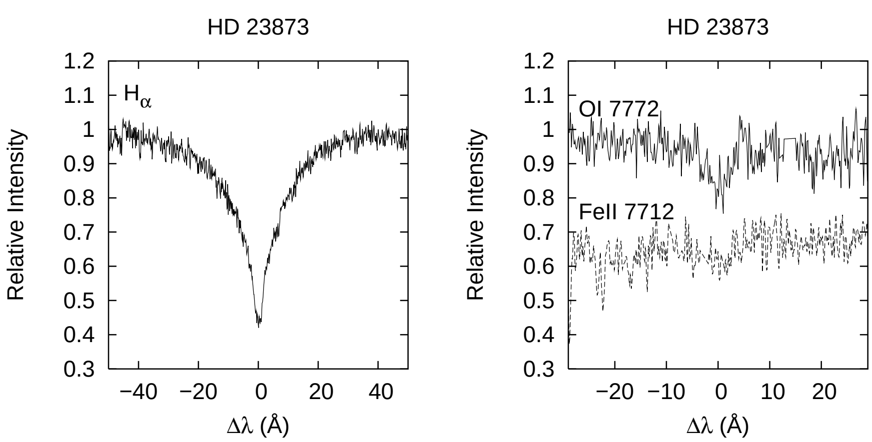

Fig. A.39. Profiles of Hα, Fe II 7712 Å, and O I 7772−5 Å lines of HD 23873.

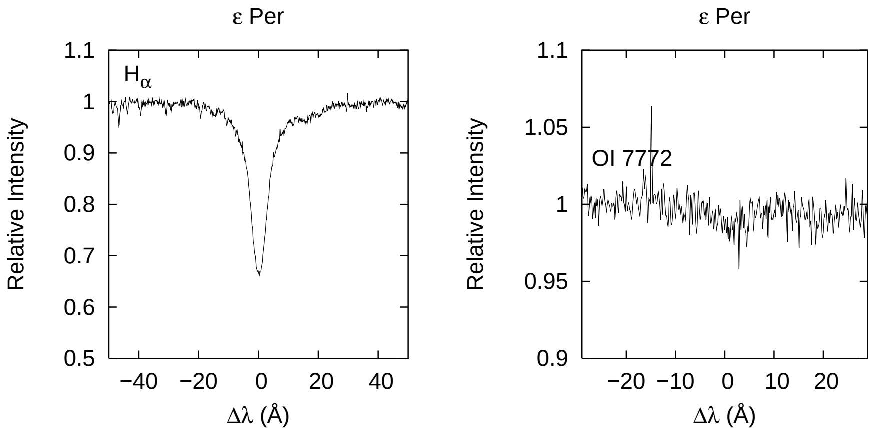

Fig. A.40. Profiles of Hα, Fe II 6516 Å, and O I 7772−5 Å lines of ε Per.

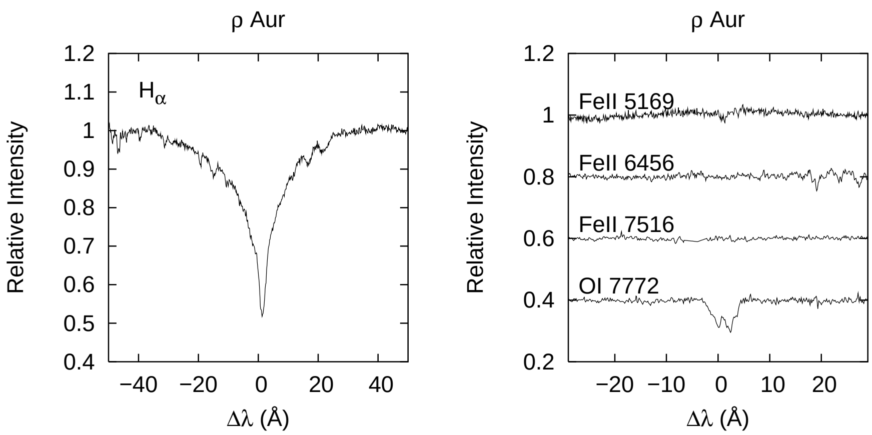

Fig. A.41. Profiles of Hα, Fe II 5169, 6456, 7516, and O I 7772−5 Å lines of ρ Aur.

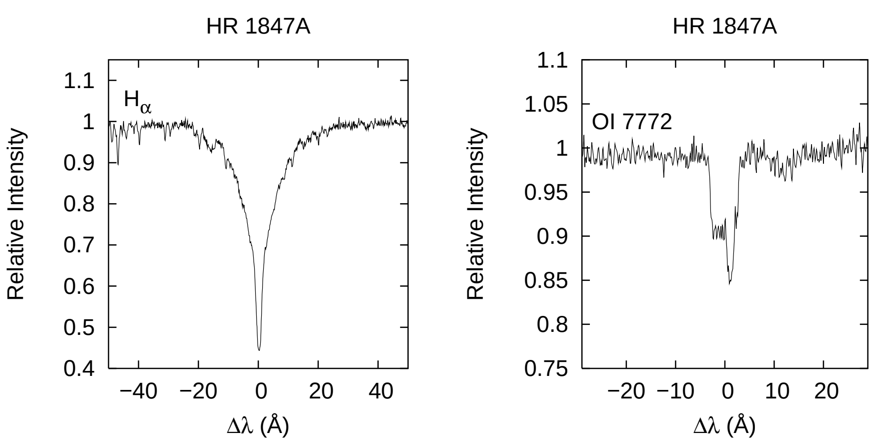

Fig. A.42. Profiles of Hα and O I 7772−5 Å lines of HR 1847A.

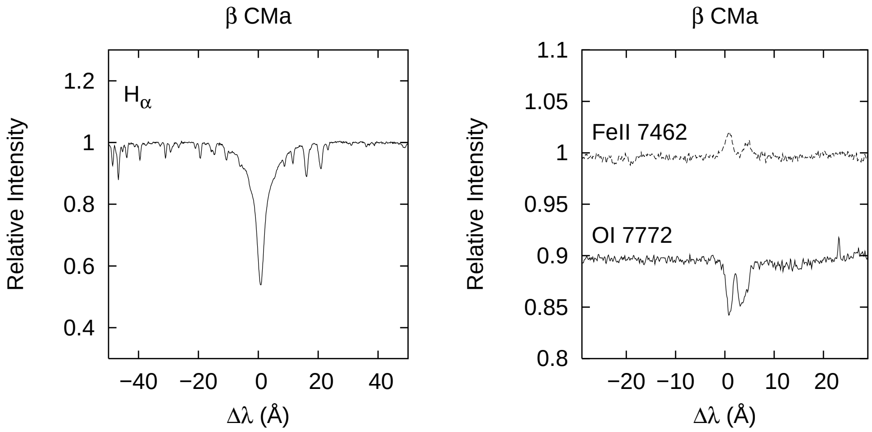

Fig. A.43. Profiles of Hα, Fe II 7462 Å, and O I 7772−5 Å lines of β CMa.

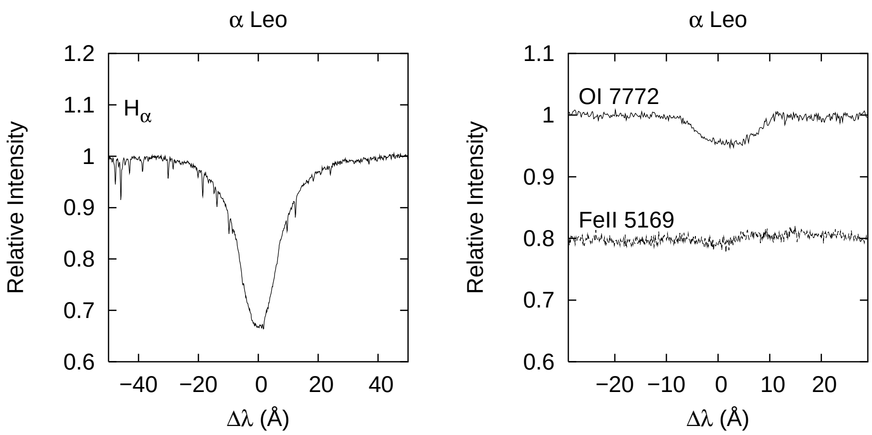

Fig. A.44. Profiles of Hα, Fe II 5169 Å, and O I 7772−5 Å lines of α Leo.

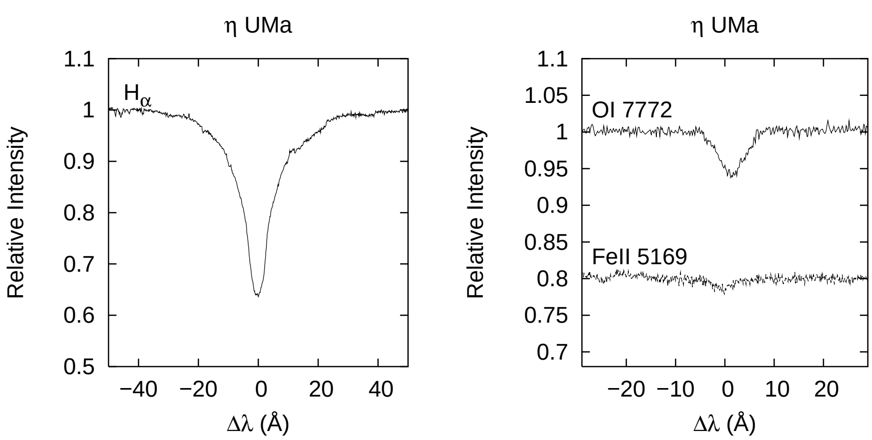

Fig. A.45. Profiles of Hα, Fe II 5169 Å, and O I 7772−5 Å lines of η UMa.

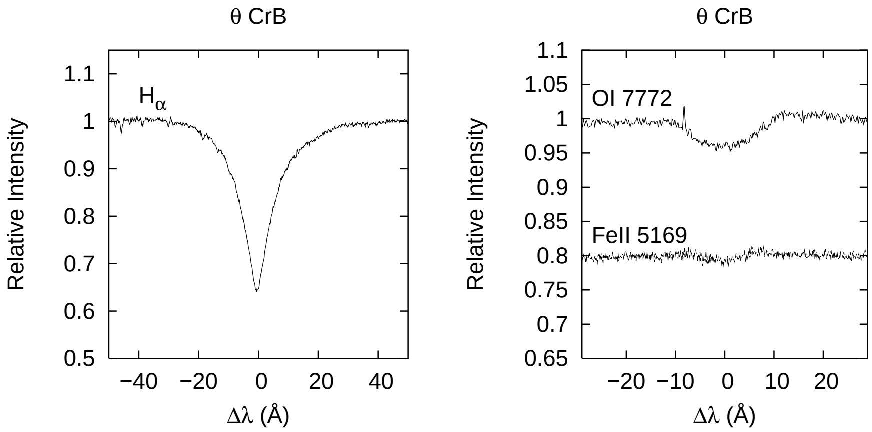

Fig. A.46. Profiles of Hα, Fe II 5169 Å, and O I 7772−5 Å lines of θ CrB.

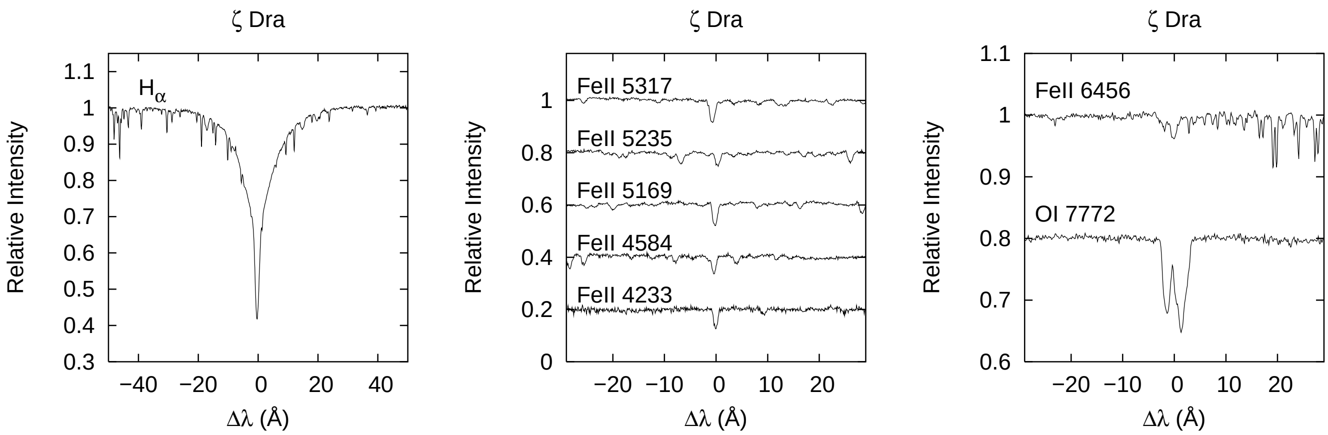

Fig. A.47. Profiles of Hα, Fe II 4233. 4584, 5169, 5235, 5317, 6456 Å and O I 7772−5 Å lines of ζ Dra.

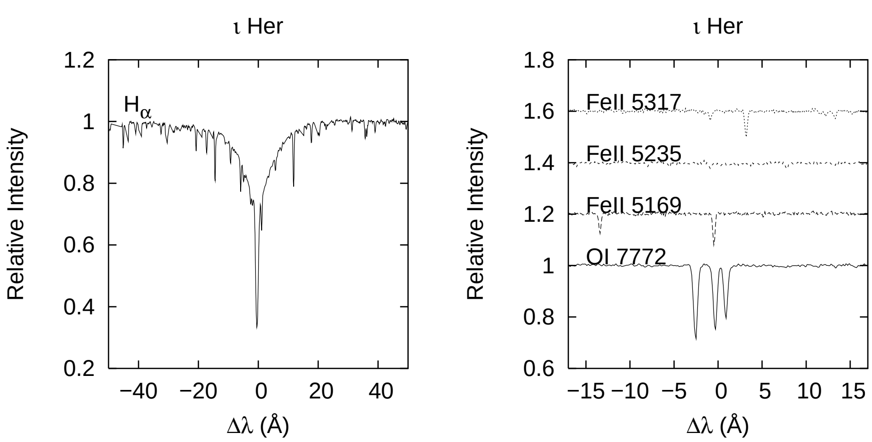

Fig. A.48. Profiles of Hα, Fe II 5169, 5235, 5317 Å, and O I 7772−5 Å lines of ι Her.

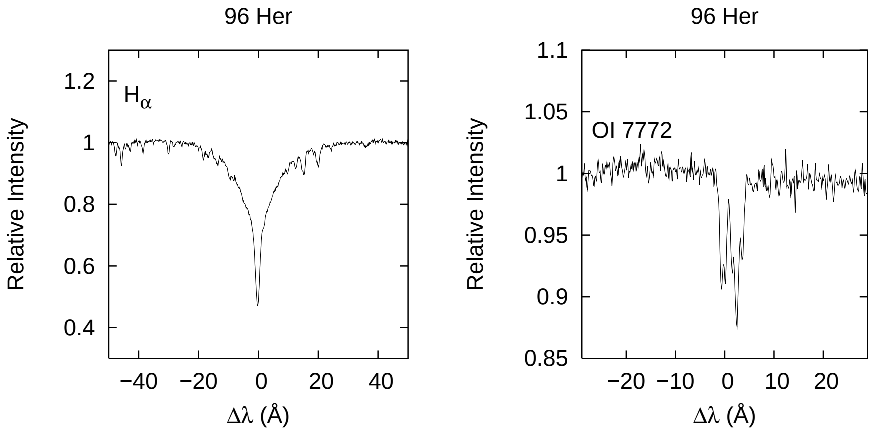

Fig. A.49. Profiles of Hα and O I 7772−5 Å lines of 96 Her.